Optimising the biosynthesis of oxygenated and acetylated Taxol precursors in Saccharomyces cerevisiae using advanced bioprocessing strategies

Walls, Laura E.; Malci, Koray; Nowrouzi, Behnaz; Li, Rachel; d'Espaux, Leo; Wong, Jeff; Dennis, Jonathan A.; Semiao, Andrea J C; Wallace, Stephen; Martinez, José L.

Total number of authors:
12

Published in:
Biotechnology and Bioengineering

Link to article, DOI:
10.1002/bit.27569

Publication date:
2021

Document Version
Peer reviewed version

Stay on the leading edge of stem cell research

The Gibco™ 5 Days of Stem Cells virtual event connects you to the latest stem cell techniques, research breakthroughs, and esteemed scientists from around the world–all from the comfort of anywhere

We'll share developments, discoveries, and cutting-edge content connected to a wide variety of stem cell applications, including disease modeling, cell and gene therapy, 3D modeling, and much more.

The 5-day virtual agenda is packed full of incredible insights in the form of:

- Leading scientific presentations from thought leaders around the world
- Behind-the-scenes virtual training demos
- Scientific poster sessions
- Hundreds of key stem cell tools and resources
- A global network of researchers including our stem cell experts and technical support

It's all happening October 12–16, 2020.

CURRENT PROTOCOLS
A Wiley Brand

Register for free at **thermofisher.com/5daysofstemcells**

ThermoFisher
SCIENTIFIC

Laura Walls ORCID iD: 0000-0002-9379-3593

Optimising the biosynthesis of oxygenated and acetylated Taxol precursors in *Saccharomyces cerevisiae* using advanced bioprocessing strategies

Laura E. Walls[a,b,g], Koray Malci[a,b+], Behnaz Nowrouzi[a,b+], Rachel Li[c,d+], Leo d'Espaux[c,d], Jeff Wong[c,d], Jonathan A. Dennis[b,e], Andrea J.C. Semiao[f], Stephen Wallace[b,e], José L. Martinez[g], Jay D. Keasling[c,d,h-j], Leonardo Rios-Solis[a,b*]

[a] *Institute for Bioengineering, School of Engineering, University of Edinburgh, Kings Buildings, Edinburgh, United Kingdom*

[b] *Centre for Synthetic and Systems Biology (SynthSys), University of Edinburgh, Kings Buildings, Edinburgh, United Kingdom*

[c] *DOE Joint BioEnergy Institute, Emeryville, California, CA 94608, USA*

[d] *Biological Systems and Engineering Division, Lawrence Berkeley National Laboratory, Berkeley, California, CA 94720, USA*

[e] *Institute for Quantitative Biology, Biochemistry and Biotechnology, School of Biological Sciences, University of Edinburgh, Kings Buildings, Edinburgh, United Kingdom*

[f] *Institute for Infrastructure and Environment, School of Engineering, University of Edinburgh, Edinburgh, EH9 3DW, UK*

This article has been accepted for publication and undergone full peer review but has not been through the copyediting, typesetting, pagination and proofreading process, which may lead to differences between this version and the Version of Record. Please cite this article as doi: 10.1002/bit.27569.

[g]*Department of Biotechnology and Biomedicine, Section for Synthetic Biology, Technical University of Denmark, Kongens Lyngby, Denmark*

[h]*Departments of Chemical & Biomolecular Engineering and of Bioengineering, University of California, Berkeley, Berkeley, CA 94720*

[i]*Center for Biosustainability, Danish Technical University, Lyngby, Denmark*

[j]*Center for Synthetic Biochemistry, Institute for Synthetic Biology, Shenzhen Institutes for Advanced Technologies, Shenzhen, China*

[+] KM, BN and RL contributed equally as second authors

**Corresponding author: Dr Leonardo Rios Solis (E -mail: Leo.Rios@ed.ac.uk; Telephone: +441316513561)*

Abstract

Taxadien-5α-hydroxylase and taxadien-5α-ol O-acetyltransferase catalyse the oxidation of taxadiene to taxadien-5α-ol and subsequent acetylation to taxadien-5α-yl-acetate in the biosynthesis of the blockbuster anti-cancer drug, paclitaxel (Taxol®). Despite decades of research, the promiscuous and multispecific CYP725A4 enzyme remains a major bottleneck in microbial biosynthetic pathway development. In this study, an interdisciplinary approach was applied for the construction and optimisation of the early pathway in *Saccharomyces cerevisiae*, across a range of bioreactor scales. High-throughput microscale optimisation enhanced total oxygenated taxane titre to 39.0±5.7 mg/L and total taxane product titres were comparable at micro and mini-bioreactor scale at 95.4±18.0 and 98.9 mg/L, respectively. The introduction of pH control successfully mitigated a reduction of oxygenated taxane production, enhancing the potential taxadien-5α-ol isomer titre to 19.2 mg/L, comparable to the

23.8±3.7 mg/L achieved at microscale. A combination of bioprocess optimisation and increased GC-MS resolution at 1L bioreactor scale facilitated taxadien-5α-yl-acetate detection with a final titre of 3.7 mg/L. Total oxygenated taxane titres were improved 2.7-fold at this scale to 78 mg/L, the highest reported titre in yeast. Critical parameters affecting the productivity of the engineered strain were identified across a range of scales, providing a foundation for the development of robust integrated bioprocess control systems.

Graphical Abstract

An interdisciplinary approach was applied for the construction and optimisation of the early stages of a Taxol biosynthetic pathway in *Saccharomyces cerevisiae*, across a range of bioreactor scales. Through design of experiments guided high-throughput microscale screening, titres of early precursors were enhanced. Critical parameters affecting productivity were identified across a range of scales. Strategic optimisation and control of such parameters at 1L bioreactor scale facilitated detection of the third Taxol intermediate, taxadien-5α-yl-acetate, under industrially relevant conditions.

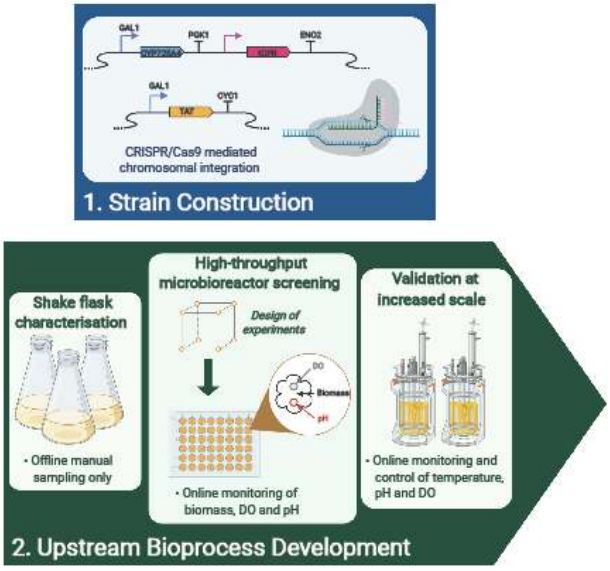

Keywords:

S. cerevisiae, Taxadien-5α-hydroxylase, High throughput microbioreactor, Taxol, Taxadien-5-alpha-ol O-acetyltransferase

Introduction

Paclitaxel (Taxol®) is one of the most widely administered chemotherapeutic agents owing to its effectiveness against a vast range of diseases. Although it is found naturally in the bark of Pacific Yew (*Taxus brevifolia*), the destruction of three mature trees is necessary to yield just one gram of paclitaxel (McElroy & Jennewein, 2018), rendering direct extraction unsustainable. Heterologous expression of the complex biosynthetic pathway using a fast-growing eukaryotic host could provide a sustainable solution. However, the pathway is yet to be fully elucidated and low and variable titres of the early precursors have been achieved to date (Liu, Gong, & Zhu, 2016; McElroy & Jennewein, 2018).

The first committed step in paclitaxel biosynthesis involves the cyclisation of geranylgeranyl diphosphate (GGPP), a product of the mevalonate pathway, by taxadiene synthase (TASY), yielding taxa-4(5),11(12)-diene (taxadiene) and its structural isomer taxa-4(20),11(12)-diene (iso-taxadiene) as shown in Figure 1.

Both compounds are substrates for the subsequent enzyme taxadien-5α-hydroxylase (CYP725A4), which is the first of several cytochrome P450s in the paclitaxel pathway (Jennewein, Long, Williams, & Croteau, 2004). The desired product of this first oxidation reaction is taxadien-5α-ol (T5αol), which subsequently undergoes acetylation in the third step in the pathway in a reaction catalysed by taxadien-5-alpha-ol O-acetyltransferase (TAT), yielding taxa-4(20),11-dien-5α-yl acetate (Walker et al. 2000).

Heterologous expression of *TASY* and *CYP725A4* has been accomplished using both *S. cerevisiae* (DeJong et al., 2006; Edgar et al., 2016) and *E. coli* (Edgar et al., 2016; Sagwan-Barkdoll & Anterola, 2018; Yadav, 2014). Although, taxadiene titres of up to

1 g/L have been achieved in *E. coli,* when *CYP725A4* was subsequently expressed in the respective strain, a significant drop in productivity was observed, with a total oxygenated taxane titre of 116 mg/L (Ajikumar et al., 2010). An impressive effort was made to optimise P450 expression and reductase partner interactions in *E. coli,* achieving a fivefold improvement in total oxygenated taxanes to 570 mg/L (Biggs et al., 2016). However, the overexpression of the subsequent cytochrome P450s in the paclitaxel pathway is likely to be very challenging in the prokaryotic host. On the other hand, the eukaryotic host, *S. cerevisiae,* possesses the necessary biosynthetic and redox capabilities for the expression of such enzymes (Engels et al., 2008). Despite this, the maximum reported taxadiene titres are eightfold lower in yeast (Nowrouzi et al., 2020). Distributing the early Taxol metabolic pathway among *E. coli* and *S. cerevisiae* facilitated a total oxygenated taxane titre of 33 mg/L (Zhou, Qiao, Edgar, & Stephanopoulos, 2015).

Microbial expression of CYP725A4 has resulted in a wide range of side products including OCT and iso-OCT (Figure 1) and the desired T5αol compound was a minor product when expressed in *E. coli* (Sagwan-Barkdoll & Anterola, 2018). Additional studies reported further unknown monooxygenated and dioxygenated taxane compounds (Edgar et al., 2016; Yadav, 2014). In addition to variations in the nature of the oxygenated taxanes produced, the ratios of the products generated differed substantially. Edgar et al. (2016) reported that T5αol comprised between 0-25% of the products of CYP725A4 depending on the microbial host, growth medium and extraction procedure used. Variations in process conditions between these steps may contribute to the observed product distributions. Despite extensive improvements in the microbial expression of the first two enzymes in the paclitaxel biosynthetic pathway, progress toward construction of the third step has been limited. Early

characterisation studies revealed taxadien-5-alpha-ol-O-acetyltransferase (TAT) is also multi-specific (K. Walker et al., 1999). Several isoprenoid alcohols including GGOH and farnesol were found to be substrates of the enzyme. Despite this, when *TAT* was heterologously expressed along with *TASY* and *CYP725A4* in *E. coli,* of the several mono and dioxygenated CYP725A4 products, only T5αol appeared to undergo acetylation (Edgar et al., 2016).

Traditionally, simple small scale shake flask or microplate cultures have been exploited for early stage bioprocess development (P. M. Doran, 1995; Funke et al., 2010). However, such systems offer limited insight to the nature of the process and there are major discrepancies in cultivation strategies across scales (Funke et al., 2010). As a result, their use has often resulted in the selection of suboptimal production conditions, leading to setbacks at the manufacturing stage (Yu et al., 2014). Maximising process understanding during the earliest stages of bioprocess development is essential to overcome such issues. In order to tackle this, scalable high-throughput screening systems have been developed, allowing industrial bioreactor conditions to be more closely mimicked (Back, Rossignol, Krier, Nicaud, & Dhulster, 2016; Funke, Diederichs, Kensy, Müller, & Büchs, 2009; Kensy, Zang, Faulhammer, Tan, & Büchs, 2009; Kostov, Harms, Randers-Eichhorn, & Rao, 2001). Through coupling such instruments with a strategic design of experiments approach, factors can be manipulated in order to statistically determine relationships between parameters and performance, ensuring quality by design.

This study aimed to develop a robust bioprocess for paclitaxel precursor production using *S. cerevisiae* microbial cell factories. State of the art micro and mini-bioreactor tools were subsequently employed to characterise and optimise the

pathway for the production of oxygenated paclitaxel precursors across a range of scales for the first time. Design of experiment strategies were applied to rapidly determine the key factors affecting productivity at microscale, whilst minimising time and resource costs. Optimal conditions were then validated using novel scale down bench-top bioreactors accelerating progress towards paclitaxel biosynthesis.

Materials and methods

Strain construction

The parent *S. cerevisiae* strain used in this study, *LRS5* {*MATa, leu2-3, 112::HIS3MX6-GAL1p-ERG19/GAL10p-ERG8;ura3-52::URA3-GAL1p-MvaSA110G/GAL10p-MvaE (codon optimised); his3Δ1::hphMX4-GAL1p-ERG12/GAL10p- IDI1; trp1-289::TRP1_GAL1p-CrtE(X.den)/GAL10p-ERG20;YPRCdelta15::NatMX-GAL1p-CrtE(opt)/GAL10p-CrtE; ARS1014::GAL1p-TASY-GFP; ARS1622b::GAL1p-MBP-TASY-ERG20; ARS1114a::TDH3p-MBP-TASY-ERG20*} was originally derived from laboratory strain CEN.PK2-1C (EUROSCARF, Germany) and has been described in more details elsewhere (Nowrouzi et al., 2020; Reider Apel et al., 2016). Strain *LRS6* was constructed through the addition of gene sequences encoding CYP725A4, its cognate cytochrome P450 reductase (*CPR*) enzyme and TAT obtained from *Taxus cuspidata*. The synthetic genes were codon optimised for *S. cerevisiae* expression and synthesised by Integrated DNA Technologies (Iowa, USA). The resulting sequences, all required primers, and single guide RNA (sgRNA) oligonucleotides were also synthesised by Integrated DNA Technologies (Iowa, USA). Chromosomal integration of transcriptional units was achieved using a cloning-free, Cas9-aided, homologous recombination method as reported by (Reider Apel et al., 2016). In summary, 2μ plasmids expressing both Cas9 and the selected sgRNA were used. The URA3

selection marker, carried by the plasmid facilitated successful transformant selection on CSM-Ura medium agar plates. For verification of genomic integrations, Sanger sequencing (Edinburgh Genomics, UK) and Next Generation Sequencing (NGS) were used. MinION NGS platform (Oxford Nanopore Technologies) was used for whole genome sequencing along with the rapid library preparation kit, SQK-RAD004. Bioinformatics analysis was carried out by using pomoxis and medaka software and Python. Transformation was performed according to the LiAc/SS carrier DNA/PEG method (Gietz & Schiestl, 2007). All chemicals were purchased from Fisher Scientific, UK at the highest available purity unless otherwise stated.

Shake flask cultivations

The *LRS6* strain weas cultivated in 250 mL Erlenmeyer flasks for three days. Inocula preparation was achieved by transferring single colonies to 5 mL of rich YPD medium (1% yeast extract; 2% peptone; 2% glucose) and incubating at 30°Cand 250 rpm overnight. Aliquots of each pre-culture were subsequently diluted with YP supplemented with 2% galactose to yield a 20 mL culture with initial OD_{600} = 1. A 20% dodecane overlay was added to give a final working volume of 25 mL. Duplicate measurements of biomass were performed for triplicate shake flasks twice daily. Taxane production was analysed via GC-MS at the end of the cultivation.

Microscale high-throughput bioreactors

For the high-throughput screening, a BioLector Pro (mp2-labs, Germany) microbioreactor-screening platform was utilised. The microbial cultures were performed in triplicate in YP medium supplemented with one of eight sugar solutions (Table 1), each representing one of the conditions explored. Inocula were prepared as described for the shake flasks. Aliquots of the appropriate pre-culture were diluted 8-

fold to a volume of 800 µL in each well with the medium indicated in the experimental design (Supplementary Table 3). A 200-µL dodecane overlay was also added to each well giving a total working volume of 1 mL. The temperature was maintained at 30°C under agitation of 1000 rpm with a shaking diameter of 3 mm in 48-well FlowerPlates (mp2-labs, Germany). Temperature, biomass, dissolved oxygen (DO) and pH were monitored online using the inbuilt optical sensors. Taxane production was analysed via GC-MS at the end of the cultivation.

Bioreactor conditions

Larger scale cultivations were conducted in MiniBio500 bioreactors (Applikon Biotechnology, The Netherlands) with a working volume of 250 mL or 1L BIOSTAT Q plus bioreactors (Sartorius-Stedim Biotech S.A, Germany) with a working volume of 500 mL. Pre-inoculum cultures were prepared by transferring from a single colony to 5 mL of YPD and incubating at 30°C and 250 rpm for eight hours. The resulting culture was subsequently used to inoculate a secondary culture to an OD_{600} = 1 and incubated overnight. An aliquot of the resulting culture was diluted with 2% (*w/v*) galactose medium to give a 200 (MiniBio 500) or 400 mL (BIOSTAT) culture with an initial OD_{600} = 1.

To prevent excess foam production polypropylene glycol P2000 (Alfa Aesar, UK) was added to a concentration of 0.01% (*v/v*) and a Rushton turbine was placed at the medium-air interface. A 20% dodecane overlay was also added. Temperature, DO and pH were measured online. The adaptive my-control system (Applikon Biotechnology, The Netherlands) was used to control process parameters in the MiniBio 500 bioreactors. A setpoint of 30% saturation for DO was applied and the culture temperature was maintained at 30°C. Where pH control was implemented, pH was

maintained above six through the automatic addition of 1M NaOH. Where biomass was measured online, a BE2100 OD scanner (BugLab, USA) was employed, and offline measurements were performed twice daily using a Nanodrop 2000c spectrophotometer (Thermo Fisher Scientific, UK). MFCS software (Version 3.0, Sartorius-Stedim Biotech S.A, Germany) was employed to control the BIOSTAT cultivation, pH was maintained at six through the automatic addition of 2M NaOH or 2M H_2SO_4 and temperature was maintained at 30^{o}C. A constant airflow of 1 vvm was maintained and stirrer speed was adjusted to maintain dissolved oxygen above 30%. Off-gas analysis was performed online via mass spectrometry (Prima Pro, Thermo Fisher Scientific, UK). Samples were taken twice daily for taxane and metabolite quantification via GC-MS and HPLC.

Taxane and metabolite identification and quantification

Taxane identification and quantification was achieved via GC-MS. The organic dodecane layer was separated from the culture medium through centrifugation and a 1-µL sample was injected into a TRACE™ 1300 Gas Chromatograph (Thermo Fisher Scientific, UK) coupled to an ISQ LT single quadrupole mass spectrometer (Thermo Fisher Scientific, UK). Chromatographic separation was achieved using a Trace Gold TG-SQC gas chromatography column using a previously described method (Nowrouzi et al., 2020). To identify and quantify production of compounds by *LRS5* and *LRS6* (Supplementary Figure 1), pure standards of taxadiene, kindly supplied by Baran Lab (The Scripps Research Institute, California, USA) and GGOH, obtained from Sigma Aldrich (Gillingham, UK), were used. Additional product concentrations were estimated relative to standard taxadiene concentrations. In the BIOSTAT cultivation, ethanol, acetate and glycerol production were analysed via ion-exchange HPLC. Following filtration using a 0.45-µm filter, 20-µL samples were injected into a

Bio-Rad Aminex HPX-87H column (Hercules, CA, United States) for analysis. The eluent was 5 mM H_2SO_4, flowrate 0.6 mL/min and the temperature was 60°C. A RID-detector was used for quantification.

Statistical analysis

Design of experiments and statistical analyses were performed using Minitab 17 statistical software. Balanced analysis of variance (ANOVA) was used to determine whether investigated factors yielded a significant impact on measured variables in the microscale yeast cultures. The null hypothesis considered that there was no significant difference between the cultures, hence if $p \leq 0.05$ the null hypothesis was rejected. The Pearson's correlation coefficient was used to assess for linear relationships between variables.

Results and discussion

Strain construction

Taxadiene synthesis is the first committed step in the Taxol biosynthetic pathway and has been achieved in batch cultivation of *S. cerevisiae* with maximum taxadiene titres of 129 and 57 mg/L at 20°C and 30°C, respectively (Nowrouzi et al., 2020). The oxygenation step in the microbial host was achieved in this study through the chromosomal integration of *Taxus cuspidata* CYP725A4 and CPR genes in tandem into locus 511b. The TAT gene, also originating from *T. cuspidata*, was integrated into locus RKC3 to construct the subsequent acetylation step. In the native host genome, locus 511b is located in chr V: 175.892 - 175.911 on the forward strand, locus RKC3 is located in chr III: 119.278 - 119.313 on the forward strand and both of the loci are in intergenic regions. The GAL1 promoter was selected to maximise expression for both CYP725A4 and TAT. Expression of the CPR enzyme has been

shown to be typically ~15-fold lower in its native host (Jensen & Møller, 2010), as disruption of the degree of coupling between the CPR and P450 enzymes increases the generation of toxic reactive oxygen species (Zangar, Davydov, & Verma, 2004). To minimise this effect, a single copy of *CPR* was expressed under the weaker GAL3 promoter. Zhou et al. (2015) highlighted the acetylation step by TAT to be the bottleneck of the early pathway, therefore the stronger GAL1 promoter was also selected for this gene as well as terminator CYC1. The construction of the genetic parts integrated into the chromosome of *LRS6* is shown in Figure 2.

Shake flask cultivation performance and enzyme characterisation

To facilitate preliminary product and growth profile characterisation, the constructed *LRS6* strain was grown in shake flask cultures were the biomass kinetics and final product profile shown in Figure 3A.

Biomass accumulation by *LRS6* reached a final OD_{600} of 22.0 ± 1.6 after 71 hours of culture, cultivation of the parent *LRS5* strain under the same experimental conditions resulted in a substantially higher OD_{600} of 36.0 ± 1.8 in just 48 hours (Supplementary Figure 2). In a similar previous study, *LRS5* biomass accumulation was also found to be 40% higher in shake flask culture (Nowrouzi et al., 2020). The reduced growth rate observed in the *LRS6* strain is therefore likely to be associated with the increased oxidative stress associated with the expression of the additional enzymes. A similar effect was observed when the *CYP725A4* and cognate *CPR* genes were incorporated into an optimised taxadiene-producing *E. coli* strain, biomass accumulation declined by over 50% (Ajikumar et al., 2010).

GC-MS analysis of the dodecane extracts from *LRS6* cultures in this study confirmed the functional expression of both the *TASY* and *CYP725A4* genes as shown

in Figure 3A and Supplementary Figure 7A. A total of six oxygenated products were produced by the strain in addition to the TASY products. The peaks at 8.34, 8.57 and 8.71 minutes were identified as iso-OCT, OCT and T5αol through comparison of the gas chromatographs and mass spectra (Supplementary Figure 5 and 6) to those reported in literature (Edgar et al., 2016; Sagwan-Barkdoll & Anterola, 2018). When expressed in *E. coli,* OCT and iso-OCT were previously found to be the major products of *CYP725A4* (Edgar et al., 2016; Sagwan-Barkdoll & Anterola, 2018; Yadav, 2014). In this study, however, a novel oxygenated diterpenoid with a retention time of 8.49 minutes (Diterpenoid 1, Supplementary Figure 7A) was the major product with a titre of 7 ± 0.2 mg/L. The mass spectrum for this compound showed a high level of similarity to that of T5αol (Supplementary Figure 5), suggesting isomerism, however, further characterisation is necessary to confirm this. An additional unknown oxygenated diterpenoid compound was eluted after 10.03 minutes (Diterpenoid 2, Supplementary Figure 7A) with characteristic peaks at m/z 55, 105, 138, 273 and 288 (Supplementary Figure 6). The CYP725A4 enzyme, like many cytochrome P450 enzymes, has been shown to be multi-specific in addition to highly promiscuous. The enzyme's activity on taxadiene, iso-taxadiene and at least one mono-oxygenated taxane has been reported (Edgar et al., 2016; Jennewein et al., 2004; Yadav, 2014). An additional component was eluted at 9.41 minutes with a molecular ion (M^+) peak (m/z) of 304. This was equivalent to taxadiene (M_r = 272 g/mol) plus O_2 (M_r = 32 g/mol) and was therefore tentatively identified as a taxadiendiol.

The nature of the majority of the side-products generated from *CYP725A4* was similar to those previously reported (Edgar et al., 2016; Sagwan-Barkdoll & Anterola, 2018; Yadav, 2014). However, the appearance and predominance of a potential T5αol

isomer (Diterpenoid 1) was novel. The expected TAT product, taxa-4(20),11-dien-5α-yl acetate (T5αAc), was not detected. This was believed to be due to insufficient substrate availability as the maximum T5αol titre achieved under these conditions was just 1 ± 0.1 mg/L. Subsequent experiments therefore focussed on the overproduction of the taxadiene and T5αol precursors.

Microscale high throughput optimisation

To maximise process insight and understanding, the BioLector Pro (mp2-labs, Baesweiler, Germany) microbioreactor-screening platform was coupled with a design of experiments approach for the high-throughput screening of bioprocessing conditions. A multilevel full factorial experiment was employed to analyse the effects of three key factors on taxane accumulation: yeast strain, total sugar concentration and glucose content (Supplementary Table 3). Both yeast strains were initially cultivated at two different total sugar concentrations, 2% and 4%, to evaluate the effect of sugar concentration and overflow metabolism on the production of taxanes. As the overexpression of the native mevalonate pathway and heterologous expression of *TASY*, *CYP725A4*, *CPR* and *TAT* relied on GAL promoters, the addition of galactose was required for taxane production. In this study, *LRS5* and *LRS6* were cultivated in pure galactose along with 10:90 and 50:50 mixtures of glucose and galactose to determine the optimum for biomass and taxane accumulation. The bioreactor results and final product profile of the high-throughput microscale screening are summarised in Figures 4 and 5 respectively.

Microscale biomass kinetics

It can be clearly seen in Figure 4A that when sugar concentration was increased from 2% to 4% for the TASY strain (*LRS5*), a significant increase in final OD_{600} was

observed from 47.8 ± 4.2 to 70.4 ± 5.6, respectively. A similar effect was seen in the *LRS6* cultures; however, as in the shake flask cultivations (Figure 3), the final biomass concentrations were lower than for the *LRS5* cultures, at 42.3 ± 1.3 and 54.3 ± 7.2 for 2% and 4% sugar cultures, respectively due to the expression of *CYP725A4, CPR* and *TAT*. Supplementation of the cultures with glucose resulted in no significant improvement in final biomass yield for both strains under all conditions tested. As expected, the rate of growth for the pure galactose cultures was slower than that of equivalent glucose containing cultures with a longer cultivation time being required to reach the stationary phase of growth.

Taxane product profiles using microscale bioreactors

The *LRS5* strain produced a maximum taxadiene titre of 137 ± 5 mg/L when grown in 4% galactose (100:0) medium. This represented 1.06 and 2.5-fold improvements in taxadiene titre to 137 ± 5mg/L compared to the highest literature titres for the strain at 20 and 30°C (Nowrouzi et al., 2020). Although TASY activity has been found to be enhanced at reduced temperature (Nowrouzi et al., 2020), preliminary studies (results not shown) using *LRS6* revealed that CYP725A4 activity was dramatically reduced at 20°C compared to 30°C. In addition, both growth rate in *S. cerevisiae* (Nowrouzi et al., 2020) and CYP725A4 activity in *E. coli* (Biggs et al., 2016) have been found to be reduced at lower temperature. This study therefore focussed on strategic optimisation to ensure high taxadiene titres at 30°C. The highest concentration of oxygenated taxanes was also achieved for *LRS6* grown in the 4% galactose (100:0) medium at 51 mg/L, representing a 1.5-fold increase compared to the highest concentration reached using the *E. coli*/*S. cerevisiae* consortium system (Zhou et al., 2015). Although the qualitative nature of the *LRS6* taxane products was highly similar to those observed in the shake flask cultures, the quantitative product

profiles differed considerably between the two scales which can be clearly seen in Supplementary Figure 7A and C. Similar variations in CYP725A4 selectivity in response to changes in processing conditions, including microbial host, growth media and extraction method have been observed previously (Edgar et al., 2016). An additional compound with a retention time of 9.28 minutes was observed in the optimal BioLector cultivation (Supplementary Figure 7C and 8), showing a high degree of similarity to the published mass spectrum of geranylgeranyl acetate (GGAc) (K. Walker et al., 1999). The endogenous GGOH side-product which was observed in this study has been previously shown to be a substrate of TAT, the product of which is GGAc. The presence of GGAc here indicated potential functional expression of TAT, however, the desired TAT product, T5αAc, was still not detected.

Mixed glucose and galactose carbon sources (2% (90:10)) have been previously found to enhance production of an alternative heterologous isoprenoid, amorphadiene, in *S. cerevisiae*, (Paradise, Kirby, Chan, & Keasling, 2008). However, in this study, it can be clearly seen in Figure 5A that increasing the glucose content generally hindered production of the different oxygenated and non-oxygenated taxanes by both strains significantly. For example, when using *LRS5* with 2% *(w/v)* of carbon source with 10 and 50% of glucose content, the taxane titres declined by 28 and 90% in comparison to using pure galactose. A similar trend was observed when using 4% *(w/v)* of carbon source for the synthesis of oxygenated and non-oxygenated taxanes by *LRS5* and *LRS6*.

It was therefore concluded that pure galactose was the most appropriate carbon source for taxane production. This was expected as the GAL promoters are actively repressed by glucose and galactose is required for their induction. In addition, a

reduction in overflown metabolism may have resulted from the slower growth rate of *S. cerevisiae* on galactose (Perez-Samper et al., 2018). As taxane production relies on products of aerobic respiration, this may also contribute to higher taxane titres, however, further research is required to confirm this. Increasing the initial sugar concentration from 0.4 to 2% galactose improved *LRS5* taxadiene titres 3.5-fold. However, when the initial concentration was doubled further to 4%, an increase in taxadiene titre of just 20% was obtained. The higher sugar concentration also favoured the side reaction converting the GGPP precursor to GGOH, the titre of which increased two-fold when cultures were supplemented with 4% pure galactose in comparison to 2%. In order to maximise flux through the desired pathway and minimise undesirable endogenous product formation, the 2% pure galactose medium was selected for subsequent cultivations.

Microscale pH kinetics

Fermenting yeasts typically acidify their growth medium through a combination of proton pumping, organic acid secretion as well as carbon dioxide evolution and dissolution (M. G. Walker & Stewart, 2016). This effect was observed for the two *S. cerevisiae* strains of this study, as shown in Figure 4C and D, in cultivations supplemented with 2% or 4% sugar. Acidification occurred during the first 10 hours and was most significant in the 2% and 4% 50:50 galactose to glucose mixtures where the pH dropped to 5.9 $\pm$ 0.07 and 5.7 $\pm$ 0.02, respectively. This was expected as glucose is fermented at a faster rate than galactose by *S. cerevisiae* and organic acids such as acetic acid are secreted as side-products of fermentation (Martinez et al., 2014). Despite this, alteration of the sugar composition had no significant difference on the final pH values of the cultures supplemented with 2% or 4% sugar ($p=0.159$).

Acidification was negligible for cultures supplemented with 0.2% or 0.4% sugar, likely due to a reduced fermentative metabolism.

Microscale dissolved oxygen kinetics

High DO concentrations (>80%) were observed throughout the cultivation for all conditions explored as shown in Figure 4E and F, indicating excellent oxygen mass transfer. However, the use of organic solvents is not recommended with FlowerPlates (m2p-labs, 2019), as degradation of the DO sensor could occur. As a result, further experiments were conducted without a dodecane overlay to characterise the effect. DO concentration readings for the cultures with and without the overlay were similar with between 87% and 96% DO being maintained throughout the cultivation (Supplementary Figure 9). The high oxygen transfer rate observed was therefore likely due to use of the novel baffled FlowerPlates, which have been found to improve k_La values two-fold at 800 rpm compared to traditional round well microtiter plates (Funke et al., 2009), eliminating oxygen limitation in *S. cerevisiae* cultures.

Process validation

Scale-up of optimal microscale conditions

During high throughput microscale screening, 2% pure galactose medium was deemed optimal for maximising flux through the heterologous taxol pathway and minimising undesirable endogenous product accumulation. A scale-up of this condition was subsequently performed to predict industrial scale performance of *LRS6*. This was achieved using 500-mL benchtop MiniBio 500 bioreactors (Applikon Biotechnology, The Netherlands) with a total working volume of 250 mL, representing a 250-fold scale up. The results of this experiment are summarised in Figure 6.

The total taxane product titres at micro and mini-bioreactor scale were highly similar at 95 ± 18 and 99 mg/L, respectively. However, the final concentration of the potential T5αol isomer was reduced substantially from 24 ± 4 at microscale to 9 mg/L using the mini-bioreactor. Oxygenated taxane compounds accounted for just 21% of the total products in the bioreactor compared to 41 ± 4% at microscale. Although acidification was observed in the microscale cultivations as shown in Figure 4C and D, it was much more significant in the bioreactor cultivation (Figure 6A). This likely contributed to the poor performance observed for the synthesis of oxygentated taxanes, as the optimal pH for the membrane bound CYP725A4 has been reported to be 7.2 in its natural source, with activity dropping by 50% at pH 6.2 (Hefner et al., 1996). This may have been further exacerbated by the instability of NADPH at reduced pH, the rate of degradation of which increases as the pH decreases below 7.5, reducing electron availability and potentially the activity of the reductase enzyme (Wu, Wu, & Knight, 1986). According to a study by (Valli et al., 2005), the internal pH of *S. cerevisiae* varies with external pH. For exponentially growing cells cultivated in media buffered to pH 5.0 and 7.0, the internal pH values were around 6.3 and 7.1, respectively (Valli et al., 2005). The pH of the culture decreased from 6.6 to 4.9, suggesting that the internal pH likely dropped below 6.3. Whereas in the microscale cultures, the minimum external pH was 5.9 ± 0.1 corresponding to an internal pH of approximately 6.7. The significant drop in pH observed in the bioreactor could therefore likely be responsible for the dramatic reduction in CYP725A4 activity. As a result, pH control was deemed necessary in future runs.

The OD_{600} plateaued at 37.0 (~6.72 g/L) in the stationary phase of growth as shown in Figure 6A, this was similar to the final value of 35.5 ± 8.7 (~6.44 ± 1.58 g/L) obtained for the same medium in the microscale bioreactor (Figure 4B). The

ability of the BioLector to effectively mimic larger scale cultivation performance has been demonstrated previously by Back et al., 2016. Although oxygenated taxane titres were lower at bioreactor scale in the study, biomass and total taxane concentrations were highly comparable.

Effect of external pH

Although *S. cerevisiae* is capable of proliferating across a broad pH range, its growth rate is optimal between pH 4-6 (Narendranath & Power, 2005) and is decreased substantially above pH 8 (Peña, Álvarez, Ramírez, Calahorra, & Sánchez, 2015). As there was a significant difference in optimal pH for the enzyme and host, an additional microscale study was conducted to evaluate the effect of pH on both taxane and biomass accumulation by *LRS6* as shown in Figure 7A and B.

The initial pH of the culture medium was buffered to seven through the addition of potassium buffer, which had a negative effect on both biomass and taxane accumulation. The final OD_{600} was 15.8 ± 2.2 compared to 37.1 ± 4.4 without the buffer as shown in Figure 7A. The titres of taxadiene and novel oxygenated diterpenoid 1 were also considerably lower at 4 ± 2 and 6 ± 2 mg/L compared to 20 ± 5 and 22 ± 6 mg/L for the non-buffered cultures. The preliminary bioreactor results (Figure 6) indicated that although lower pH (<5.0) did not impair cell growth, it was detrimental to CYP725A4 activity. Higher pH (>6.5) hindered yeast growth and also led to lower oxygenated taxane titres. Although temporal monitoring of taxane accumulation was not possible at microscale due to limited culture volumes, statistical analysis of the MiniBio scale kinetics revealed a strong positive correlation between OD_{600} and taxane titre (Pearson's r = 0.8916, Figure 6). A compromise was therefore necessary to maximise both taxane and biomass accumulation. The non-buffered

culture dropped to around pH 6.0 as shown in Figure 7A and resulted in significantly higher total taxane titres. In addition, pH 6.0 has been shown to be the upper limit of the optimal range for yeast growth (Narendranath & Power, 2005). A pH of 6.0 was therefore implemented in the subsequent bioreactor cultivation, the data for which is summarised in Figure 7C and 7D. During the first 12 hours of the cultivation, a fivefold increase in biomass was observed, followed by a lag phase in the subsequent 12 hours. A similar effect was observed in the shake flask (Figure 3A) and microscale cultures (Figure 4). This lag phase is characteristic of *S. cerevisiae* cultures as the carbon source is switched from glucose to galactose. The growth observed in the initial 12 hours is therefore likely to have been the result of an additional, more preferable carbon source within the growth medium such as residual glucose from the inoculum or carbohydrates present in the complex yeast extract medium. The final OD_{600} values for the initial cultivation without pH control (Figure 6A) and subsequent controlled cultivation (Figure 7C) were comparable at 38.9 and 34.5, respectively. When the pH was controlled above six in the mini-bioreactor (Figure 7D), the total product titre was 50% lower (56.0 mg/L) than that obtained in the absence of pH control (98.9 mg/L, Figure 6B). Despite this, the titre of diterpenoid 1 increased significantly from 8.9 (Figure 6B) to 19.2 mg/L (Figure 7D), confirming increased CYP725A4 activity at higher pH. Statistical analysis confirmed a strong positive correlation between total taxane concentration and OD_{600} in the pH-controlled bioreactor (Pearson's r = 0.9625). A pH of 6 was therefore selected for subsequent cultivations to maximise accumulation of both. This highlights the importance of integrating critical process parameter control in the early stages of the design-build-test-learn cycle to ensure effective microbial cell factory construction and optimisation.

Detection of taxadien-5α-yl-acetate

GGAc was detected during the microscale optimisation study, indicating potential TAT activity, however, it was not detected in the bioreactor or shake flask cultures. TAT relies on acetyl-CoA as a substrate, a major product of aerobic respiration. One of the key advantages of the baffled FlowerPlates employed in the microscale optimisation study is excellent oxygen mass transfer (m2p-labs, 2019), which eliminated oxygen limitation. Although dissolved oxygen was controlled above 30% saturation through air sparging in the bioreactor, oxygen availability was likely reduced compared to the FlowerPlate. As galactose metabolism is respiratory-fermentative, it was hypothesised that increasing oxygen availability through constant airflow at bioreactor scale may increase flux through aerobic respiration and hence acetylated taxane production. The optimised conditions were scaled up further using highly instrumented 1L BIOSTAT bioreactors, with a constant airflow of 1 vvm, to facilitate further characterisation. The results of this experiment are summarised in Figure 8.

As in previous cultivations an initial growth phase was observed. During the first 22 hours of growth the OD_{600} increased from 1 to 14.4 (Figure 8A). Following this a lag phase was observed and ethanol production initiated. At around 48 hours, the ethanol concentration reached a maximum of 2.7 g/L (Figure 8A) and the oxygen uptake rate (OUR) began to increase (Figure 8C). This indicated a switch from predominantly fermentative metabolism of galactose to aerobic respiration. Growth proceeded via respiration of ethanol and acetate with a maximum OD_{600} of 34.6 (~6.28 g/L) being reached at around 72 hours, highly comparable to the 34.5 (~6.26 g/L) obtained in the 500 mL bioreactor (Figure 7C). The rate of biomass and taxane accumulation was greatest between 48 and 72 hours. At 72 hours the metabolizable

carbon sources, galactose, ethanol and acetate had been exhausted and the stationary phase of growth was reached (Figure 8A). In the final 48 hours of cultivation a slight increase in total taxane concentration from 154 to 171 mg/L was observed despite the cells being in the stationary phase of growth. Previous work indicated that some taxadiene may be retained intracellularly and secreted during the stationary phase of growth (Nowrouzi et al., 2020). The observed increase in taxane concentration may have therefore been the result of secreted intracellular taxanes. An alternative extraction procedure incorporating a cell lysis step could therefore allow similar titres to be achieved in a shorter cultivation time.

Closer inspection of the mass spectrum of the suspected taxadiendiol compound produced in previous cultivations (Supplementary Figure 6C) revealed peaks at m/z = 255, 270 and 287 in addition to the characteristic taxadiendiol peaks at m/z = 286 and 304. These peaks have not been reported in other taxadiendiol mass spectra, however, such peaks have been found diagnostic of T5αAc (255: P^+-CH_3COOH-CH_3, 270: P^+-CH_3COOH and 287: P^+-CH_3CO) (K. Walker et al., 1999). It was therefore further hypothesised that the two compounds may be co-eluting. According to the fundamental resolution equation, increasing the length of the chromatography column generally improves separation, therefore in this study a 30-m column was used in place of the 15-m column used in previous results. This successfully improved chromatographic separation as shown in Supplementary Figure 10B. An additional four potential diterpene and two potential diterpenoid compounds were detected (Supplementary Figure 10B & 13). The taxadiendiol peak was successfully separated into two peaks with retention times of 11.89 and 11.91 respectively, however, there was overlapping observed indicating resolution could be improved further. The mass spectrum of the compound eluted at 11.89 minutes (Supplementary Figure 11) was

almost identical to that of T5αAc published in literature (Edgar et al., 2016; K. Walker et al., 1999) with the exception of a peak at m/z = 245. The peak at 11.91 contained the diagnostic taxadiendiol peaks at m/z = 304 and 286 along with a large base peak at m/z = 245 (Supplementary Figure 12). An extracted ion chromatogram was generated for m/z=245, this revealed a large single peak at 11.91 minutes (Supplementary Figure 10A). This indicated that the peak at m/z = 245 was most likely the result of overlapping rather than the compound eluted at 11.89 minutes. The compound eluted at 11.89 minutes was therefore tentatively identified as T5αAc. Quantification was performed relative to the taxadiene standard and the resulting final T5αAc titre was 3.7 mg/L, representing a four-fold improvement in acetylated taxadiene in *S. cerevisiae* in comparison to the previous literature (Zhou et al., 2015). Diterpene 2 was not detected using the optimised GC-MS protocol, however, an additional four diterpene compounds (diterpene 3, diterpene 4, diterpene 5 and diterpene 6, Supplementary Figure 10B) were detected between taxadiene and iso-OCT. This suggests that the previously identified diterpene 2 compound may have also been two or more of the additional diterpene products co-eluting.

Comparison of the systems studied

The simultaneous expression of *TASY*, *CYP725A4*, *CPR* and *TAT* was found to be sensitive to deviations in processing conditions at different production scales. Variations in both the titre and product composition were observed as summarised in Figure 9 and Supplementary Figure 7. The results obtained using the BioLector and uncontrolled MiniBio 500 systems were highly comparable for the *LRS6* strain. The final OD_{600} values were 42.3 ± 1.3 (~7.68 ± 0.24 g/L) and 38.9 (~7.06 g/L), and the total product titres were 95 ± 18 and 99 mg/L for the micro and mini-bioreactor systems, respectively. However, both oxygenated taxane and GGOH production were

reduced in the bioreactor cultivation. The CYP725A4 enzyme was found to be very sensitive to deviations in process conditions between the two scales. To compare selectivity across the systems studied, the yield of each product as a percentage of the total products was plotted as shown in Figure 9A. The total non-oxygenated and oxygenated taxane titres were also plotted in Figure 9B. The products of most interest were iso-taxadiene, taxadiene, diterpenoid 1, T5αol and T5αAc, due to their active role in the Taxol biosynthetic pathway. Variation in selectivity towards these compounds across scales was therefore also summarised in Figure 9C.

The major products of TASY and CYP725A4 were found to be taxadiene and the novel potential T5αol isomer, diterpenoid 1, respectively, under all of the conditions explored. However, selectivity towards the minor enzymatic products varied considerably, with varying quantities of the additional side-products of the enzymes being produced as shown in Figure 9. Although the BioLector facilitated the monitoring of critical process parameters including pH and DO, control of such parameters was not practicable. This was particularly problematic for strain *LRS6* as CYP725A4 activity was found to be negatively affected by suboptimal pH. Increased acidification in the uncontrolled bioreactor cultivation resulted in a 50% reduction in oxygenated taxane titre as shown in Figure 9B, despite highly comparable overall taxane titres. Although controlling the pH to a setpoint of 6 improved oxygenated taxane titres dramatically in subsequent cultivations, the final taxadiene titres were 10 and 54 mg/L for the pH-controlled MiniBio and BIOSTAT cultivations, respectively, indicating that CYP725A4 activity could be improved further. As the enzyme performs optimally at higher pH, increasing the pH of the culture medium in the final stages of the cultivation may improve conversion of taxadiene to T5αol; however, further research is required to confirm this. A small quantity of GGAc was detected in

the BioLector cultivations indicating functional TAT expression. Through a combination of bioprocess optimisation and improved GC-MS resolution at increased scale it was possible to detect the desired T5αAc compound. The resulting cultivation incorporated the optimised 2% galactose medium, pH setpoint of 6 and constant air supply at 1 vvm leading to a maximum titre of 3.7 mg/L. The oxygenated taxane titre was also improved 2.4-fold to 78 mg/L compared to the highest reported titre for the *E. coli/S. cerevisiae* consortium system (Zhou et al., 2015). To our knowledge, this is the first time acetylated taxanes have been successfully produced in an individual *S. cerevisiae* strain.

Conclusion

In this study, critical factors affecting CYP725A4 enzymatic performance in an engineered *S. cerevisiae* strain were elucidated across a range of scales, providing a foundation for the development of robust integrated bioprocess control systems. Optimised cultivation of the engineered *S. cerevisiae* strain with three copies of taxadiene synthase (*LRS5)* in the FlowerPlates facilitated 1.06 and 2.5-fold improvements in taxadiene titre to 137 ± 5 mg/L compared to the highest literature titres for the strain at 20 and 30°C (Nowrouzi et al., 2020). In this study, strategic optimisation ensured high taxadiene titres at 30°C, thereby eliminating reliance on sub-optimal cultivation temperatures. In contrast to bacterial systems in which the by-products OCT and Iso-OCT were the major products of CY725A4 (Edgar et al., 2016), when expressed in the *S. cerevisiae* strain, a novel potential T5αol isomer (diterpenoid 1) was the predominant product with maximum titres of 24 ± 6 and 31 mg/L at micro and 1L bioreactor scale, respectively. Biomass and total taxane titres achieved using the BioLector were comparable to those achieved in the MiniBio 500 bioreactor. The online monitoring capabilities of the BioLector proved invaluable for

the primary high-throughput screening of wide-ranging processing conditions. However, as a result of the vulnerability of the complex cytochrome P450 enzyme to deviations in external processing conditions, further optimisation was essential to achieve comparable performance at an increased scale. Significant discrepancies were identified between the optimal conditions for the host and the catalytic activity of the different recombinant enzymes; therefore, a compromise was necessary to alleviate the key bottlenecks. Despite a 500-fold scale up in working volume, through careful control of critical process parameters including pH and O2, paclitaxel precursor synthesis was improved substantially at bioreactor scale in just three experimental runs. Total oxygenated taxane titres were improved two-fold to 78 mg/L and the acetylated T5αAc product was detected for the first time with a final titre of 3.7 mg/L. This highlights that maximising process insight from the earliest stages of the design-build-test-learn cycle is critical to successful bioprocess development.

Acknowledgements

The authors would like to thank Ms. Caroline Delahoyde and Mr. Martin Corcoran at The School of Engineering, University of Edinburgh, UK and Dr Aaron John Christian Andersen and Mette Amfelt at the DTU Metabolomics Core, DTU, Denmark for their kind assistance and technical support with GC-MS analysis. Thanks to Tina Johansen at the DTU Fermentation Core, DTU, Denmark for her assistance with the BIOSTAT cultivations and HPLC analyses. Thanks to Professor Phil Baran's Lab at The Scripps Research Institute, San Diego, California for providing the taxadiene standard. This work was supported by the Engineering and Physical Sciences Research Council [grant number EP/R513209/1], Ministry of National Education of the Republic of Turkey, The University of Edinburgh (Principal's Career Development PhD Scholarship), the Royal Society [grant number

RSG\R1\180345], The University of Edinburgh Global Challenges Theme Development Fund 418 [grant number: TDF_03], the US National Science Foundation (Award Number 1330914), and the Novo Nordisk Foundation within the frame of the Fermentation Based Biomanufacturing initiative [grant number: NNF17SA0031362].

Declaration of interest

J.D.K. has financial interests in Amyris, Lygos, Demetrix, Napigen, Maple Bio, Apertor Labs, Ansa Biotechnologies, and Berkeley Brewing Sciences.

Author contributions

LW designed and performed the majority of the shake flask, microscale and bioreactor experiments including all of the data analysis. LW wrote the manuscript with input from all authors. JW, LD and RL contributed with the genome engineering experiments. BN and JD contributed with preliminary microscale and shake flask experiments. KM contributed with the next generation sequencing experiments. AS provided support with GCMS analysis and reviewing the manuscript. SW assisted with mass spectrometry analysis and reviewing the manuscript. JM, JK and LR conceived and coordinated the study.

References

Ajikumar, P. K., Xiao, W.-H., Tyo, K. E. J., Wang, Y., Simeon, F., Leonard, E., … Stephanopoulos, G. (2010). Isoprenoid pathway optimization for Taxol precursor overproduction in Escherichia coli. *Science (New York, N.Y.)*, *330*(6000), 70–74. https://doi.org/10.1126/science.1191652

Back, A., Rossignol, T., Krier, F., Nicaud, J.-M., & Dhulster, P. (2016). High-

throughput fermentation screening for the yeast Yarrowia lipolytica with real-time monitoring of biomass and lipid production. *Microbial Cell Factories*, *15*(1), 147. https://doi.org/10.1186/s12934-016-0546-z

Biggs, B. W., Lim, C. G., Sagliani, K., Shankar, S., Stephanopoulos, G., De Mey, M., & Ajikumar, P. K. (2016). Overcoming heterologous protein interdependency to optimize P450-mediated Taxol precursor synthesis in Escherichia coli. *Proceedings of the National Academy of Sciences of the United States of America*, *113*(12), 3209–3214. https://doi.org/10.1073/pnas.1515826113

DeJong, J. M., Liu, Y., Bollon, A. P., Long, R. M., Jennewein, S., Williams, D., & Croteau, R. B. (2006). Genetic engineering of taxol biosynthetic genes in Saccharomyces cerevisiae. *Biotechnology and Bioengineering*, *93*(2), 212–224. https://doi.org/10.1002/bit.20694

Delic, M., Valli, M., Graf, A. B., Pfeffer, M., Mattanovich, D., & Gasser, B. (2013). The secretory pathway: exploring yeast diversity. *FEMS Microbiology Reviews*, *37*(6), 872–914. https://doi.org/10.1111/1574-6976.12020

Doran, P. M. (1995). *1 - Bioprocess Development: An Interdisciplinary Challenge* (P. M. B. T.-B. E. P. Doran, Ed.). https://doi.org/https://doi.org/10.1016/B978-012220855-3/50001-8

Edgar, S., Zhou, K., Qiao, K., King, J. R., Simpson, J. H., & Stephanopoulos, G. (2016). Mechanistic Insights into Taxadiene Epoxidation by Taxadiene-5α-Hydroxylase. *ACS Chemical Biology*, *11*(2), 460–469. https://doi.org/10.1021/acschembio.5b00767

Funke, M., Buchenauer, A., Schnakenberg, U., Mokwa, W., Diederichs, S., Mertens,

A., … Büchs, J. (2010). Microfluidic biolector—microfluidic bioprocess control in microtiter plates. *Biotechnology and Bioengineering*, *107*(3), 497–505. https://doi.org/10.1002/bit.22825

Funke, M., Diederichs, S., Kensy, F., Müller, C., & Büchs, J. (2009). The baffled microtiter plate: Increased oxygen transfer and improved online monitoring in small scale fermentations. *Biotechnology and Bioengineering*, *103*(6), 1118–1128. https://doi.org/10.1002/bit.22341

Gietz, R. D., & Schiestl, R. H. (2007). High-efficiency yeast transformation using the LiAc/SS carrier DNA/PEG method. *Nature Protocols*, *2*, 31. Retrieved from https://doi.org/10.1038/nprot.2007.13

Hefner, J., Rubenstein, S. M., Ketchum, R. E. B., Gibson, D. M., Williams, R. M., & Croteau, R. (1996). Cytochrome P450-catalyzed hydroxylation of taxa-4(5),11(12)-diene to taxa-4(20),11(12)-dien-5a-o1: the first oxygenation step in taxol biosynthesis. *Chemistry & Biology*, *3*(6), 479–489. https://doi.org/https://doi.org/10.1016/S1074-5521(96)90096-4

Jennewein, S., Long, R. M., Williams, R. M., & Croteau, R. (2004). Cytochrome P450 Taxadiene 5α-Hydroxylase, a Mechanistically Unusual Monooxygenase Catalyzing the First Oxygenation Step of Taxol Biosynthesis. *Chemistry & Biology*, *11*(3), 379–387. https://doi.org/https://doi.org/10.1016/j.chembiol.2004.02.022

Jensen, K., & Møller, B. L. (2010). Plant NADPH-cytochrome P450 oxidoreductases. *Phytochemistry*, *71*(2), 132–141. https://doi.org/https://doi.org/10.1016/j.phytochem.2009.10.017

Kensy, F., Zang, E., Faulhammer, C., Tan, R.-K., & Büchs, J. (2009). Validation of a high-throughput fermentation system based on online monitoring of biomass and fluorescence in continuously shaken microtiter plates. *Microbial Cell Factories*, *8*, 31. https://doi.org/10.1186/1475-2859-8-31

Kostov, Y., Harms, P., Randers-Eichhorn, L., & Rao, G. (2001). Low-cost microbioreactor for high-throughput bioprocessing. *Biotechnology and Bioengineering*, *72*(3), 346–352. https://doi.org/10.1002/1097-0290(20010205)72:3<346::AID-BIT12>3.0.CO;2-X

Liu, W. C., Gong, T., & Zhu, P. (2016). Advances in exploring alternative Taxol sources. *RSC Advances*, *6*(54), 48800–48809. https://doi.org/10.1039/C6RA06640B

m2p-labs. (2019). FlowerPlate - Data sheet Flowerplate.

McElroy, C., & Jennewein, S. (2018). Taxol® Biosynthesis and Production: From Forests to Fermenters. In W. Schwab, B. M. Lange, & M. Wüst (Eds.), *Biotechnology of Natural Products* (pp. 145–185). https://doi.org/10.1007/978-3-319-67903-7_7

Narendranath, N. V, & Power, R. (2005). Relationship between pH and medium dissolved solids in terms of growth and metabolism of lactobacilli and Saccharomyces cerevisiae during ethanol production. *Applied and Environmental Microbiology*, *71*(5), 2239–2243. https://doi.org/10.1128/AEM.71.5.2239-2243.2005

Nowrouzi, B., Li, R., Walls, L. E., d'Espaux, Leopold, Malci, K., Liang, L., … Rios Solis, L. (2020). Enhanced production of taxadiene in Saccharomyces cerevisiae.

BioRxiv, 2020.06.08.139600. https://doi.org/10.1101/2020.06.08.139600

Paradise, E. M., Kirby, J., Chan, R., & Keasling, J. D. (2008). Redirection of flux through the FPP branch-point in Saccharomyces cerevisiae by down-regulating squalene synthase. *Biotechnology and Bioengineering*, *100*(2), 371–378. https://doi.org/10.1002/bit.21766

Peña, A., Álvarez, H., Ramírez, J., Calahorra, M., & Sánchez, N. S. (2015). Effects of high medium pH on growth, metabolism and transport in Saccharomyces cerevisiae. *FEMS Yeast Research*, *15*(2). https://doi.org/10.1093/femsyr/fou005

Perez-Samper, G., Cerulus, B., Jariani, A., Vermeersch, L., Barrajón Simancas, N., Bisschops, M. M. M., … Verstrepen, K. J. (2018). The Crabtree Effect Shapes the Saccharomyces cerevisiae Lag Phase during the Switch between Different Carbon Sources. *MBio*, *9*(5), e01331-18. https://doi.org/10.1128/mBio.01331-18

Reider Apel, A., Sachs, D., Tong, G. J., d'Espaux, L., Wehrs, M., Garber, M., … Zhuang, W. (2016). A Cas9-based toolkit to program gene expression in Saccharomyces cerevisiae. *Nucleic Acids Research*, *45*(1), 496–508. https://doi.org/10.1093/nar/gkw1023

Sagwan-Barkdoll, L., & Anterola, A. M. (2018). Taxadiene-5α-ol is a minor product of CYP725A4 when expressed in Escherichia coli. *Biotechnology and Applied Biochemistry*, *65*(3), 294–305. https://doi.org/10.1002/bab.1606

Valli, M., Sauer, M., Branduardi, P., Borth, N., Porro, D., & Mattanovich, D. (2005). Intracellular pH distribution in Saccharomyces cerevisiae cell populations, analyzed by flow cytometry. *Applied and Environmental Microbiology*, *71*(3), 1515–1521. https://doi.org/10.1128/AEM.71.3.1515-1521.2005

Walker, K., Ketchum, R. E. B., Hezari, M., Gatfield, D., Goleniowski, M., Barthol, A., & Croteau, R. (1999). Partial Purification and Characterization of Acetyl Coenzyme A: Taxa-4(20),11(12)-dien-5α-olO-Acetyl Transferase That Catalyzes the First Acylation Step of Taxol Biosynthesis. *Archives of Biochemistry and Biophysics*, *364*(2), 273–279. https://doi.org/https://doi.org/10.1006/abbi.1999.1125

Walker, M. G., & Stewart, G. G. (2016). Saccharomyces cerevisiae in the Production of Fermented Beverages. *Beverages*, Vol. 2. https://doi.org/10.3390/beverages2040030

Wu, J. T., Wu, L. H., & Knight, J. A. (1986). Stability of NADPH: effect of various factors on the kinetics of degradation. *Clinical Chemistry*, *32*(2), 314 LP – 319. Retrieved from http://clinchem.aaccjnls.org/content/32/2/314.abstract

Yadav, V. G. (2014). Unraveling the multispecificity and catalytic promiscuity of taxadiene monooxygenase. *Journal of Molecular Catalysis B: Enzymatic*, *110*, 154–164. https://doi.org/https://doi.org/10.1016/j.molcatb.2014.10.004

Yu, L. X., Amidon, G., Khan, M. A., Hoag, S. W., Polli, J., Raju, G. K., & Woodcock, J. (2014). Understanding pharmaceutical quality by design. *The AAPS Journal*, *16*(4), 771–783. https://doi.org/10.1208/s12248-014-9598-3

Zangar, R. C., Davydov, D. R., & Verma, S. (2004). Mechanisms that regulate production of reactive oxygen species by cytochrome P450. *Toxicology and Applied Pharmacology*, *199*(3), 316–331. https://doi.org/https://doi.org/10.1016/j.taap.2004.01.018

Zhou, K., Qiao, K., Edgar, S., & Stephanopoulos, G. (2015). Distributing a metabolic

pathway among a microbial consortium enhances production of natural products.

Nature Biotechnology, *33*(4), 377–383. https://doi.org/10.1038/nbt.3095

Figure 1: Engineered biosynthetic pathway in S. cerevisiae. A) The pathway highlighted in blue is the native mevalonate pathway; a product of this is the universal diterpenoid precursor, GGPP. The first enzyme in the paclitaxel pathway (highlighted in red), TASY catalyses the conversion of GGPP yielding taxadiene and small amounts of its isomer iso-taxadiene. The second enzyme CYP725A4, coupled with its cognate reductase subsequently catalyses the oxidation of taxadiene to T5αol. The third enzyme, TAT, then catalyses the acetylation of T5αol. Native, overexpressed genes are highlighted in blue whilst heterologous genes are highlighted in red. Dashed arrows highlight undesirable side-products; the structures of the two well-characterised by-products, OCT and iso-OCT are shown

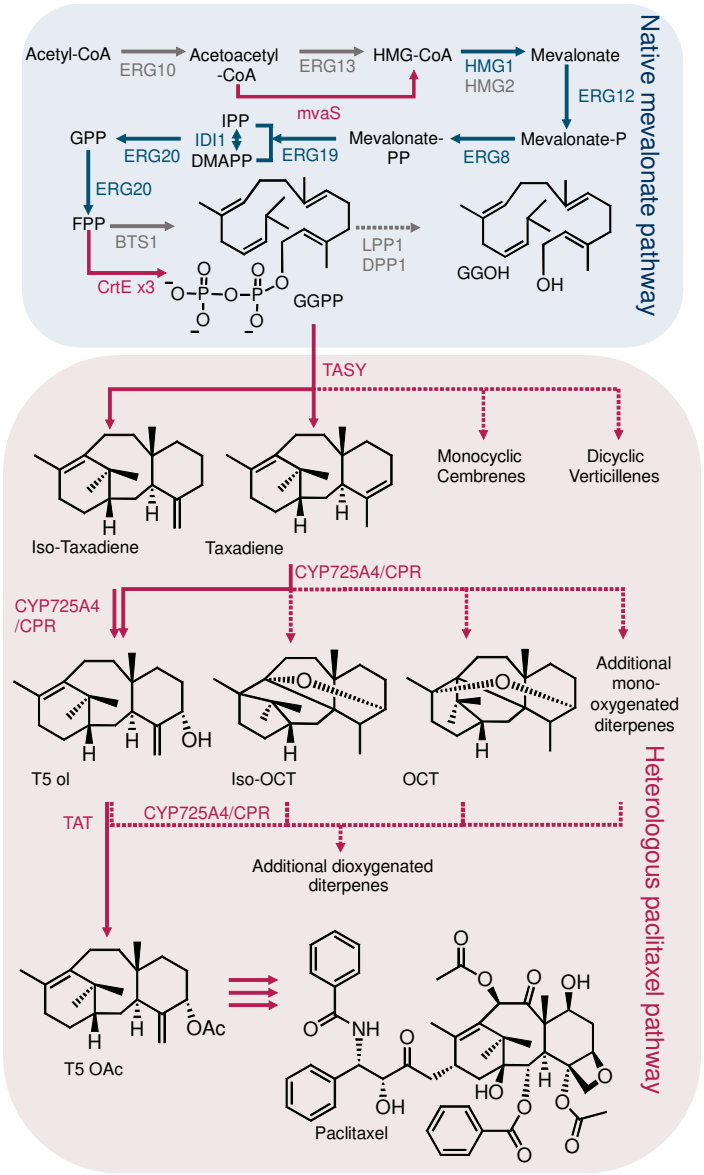

Figure 2 Construction of T5αAc pathway in S. cerevisae. Genes CYP725A4 and CPR were chromosomally integrated in tandem into locus 511b to facilitate T5αol biosynthesis. TAT was subsequently integrated into locus RKC3 for the acetylation of T5αol to T5αAc

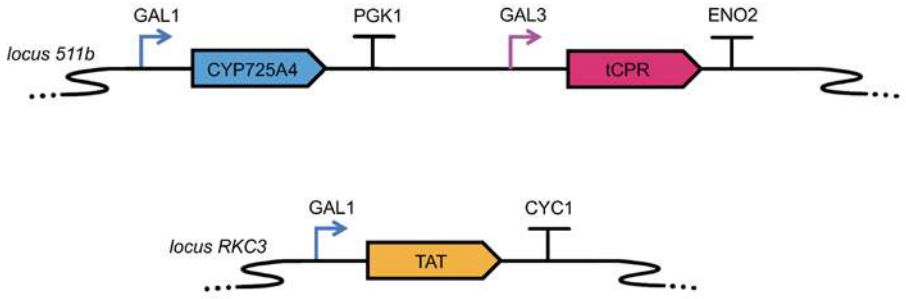

Figure 3: LRS6 growth and productivity characterisation in shake flasks. A) Plot of biomass measured as absorbance at 600nm. B) Final Taxane and GGOH titres determined via GC-MS. Values are mean ± standard deviation for triplicate shake flasks

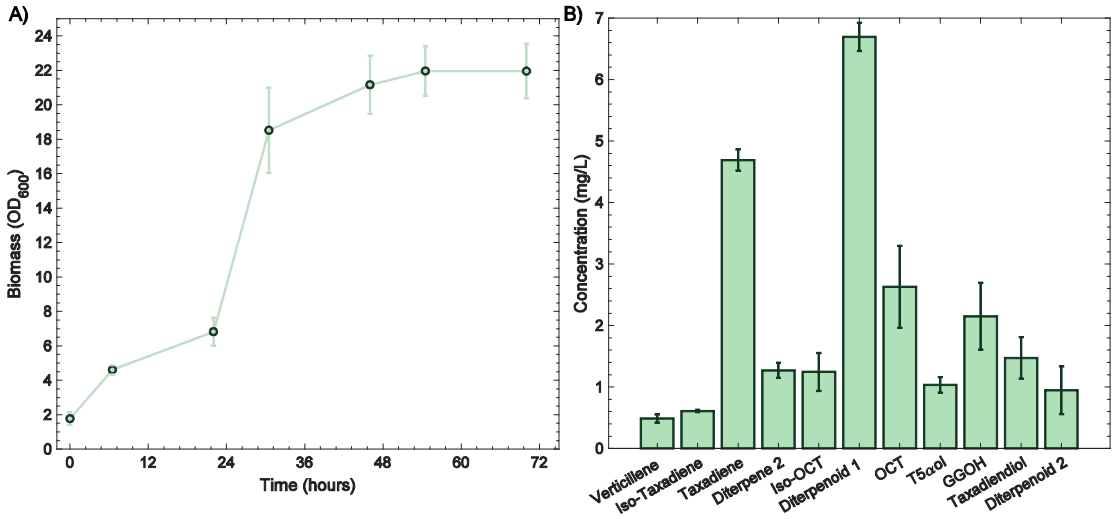

Figure 4: Online high throughput microscale screening results. Plots on the left (A, C, E) and right (B, D, F) correspond to data from LRS5 (TASY only) and LRS6 (TASY, CYP725A4, CPR and TAT) cultivations, respectively. Biomass concentration (A and B), pH (C and D) and DO concentration (E and F) were measured continuously in each well, values are mean ± standard deviation for triplicate readings. Percentage values correspond to total sugar concentration (0.2,0.4,2 or 4%) and values in parentheses correspond to galactose to glucose ratio

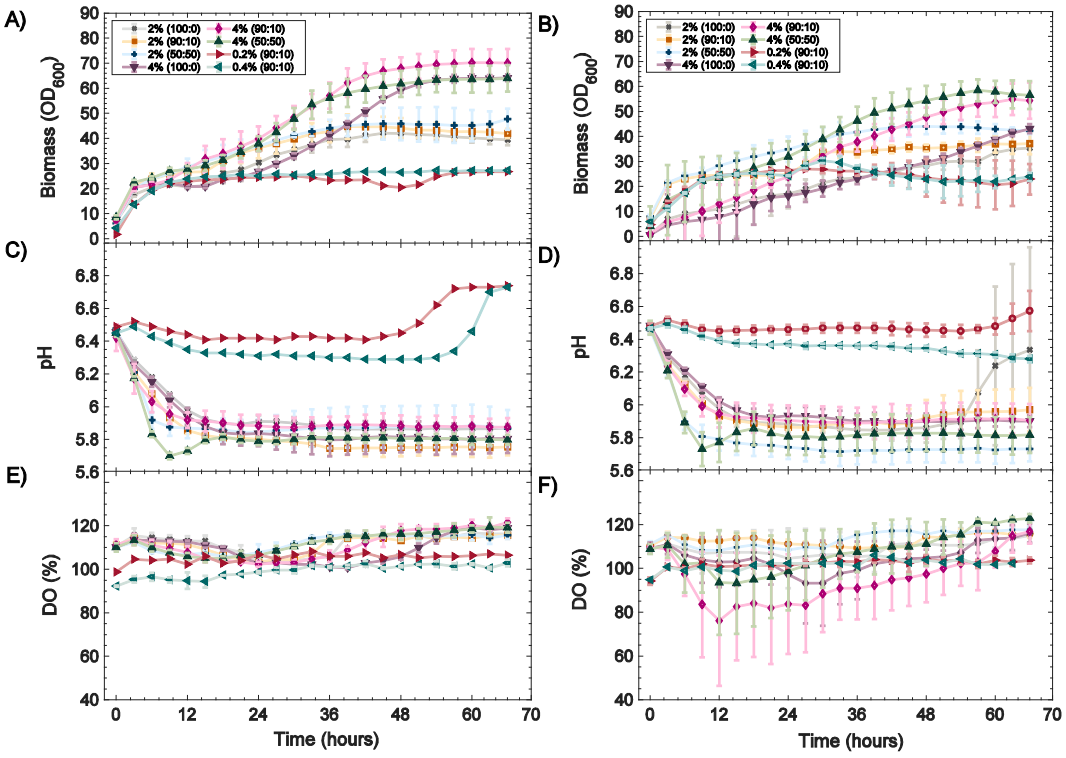

Figure 5: Taxanes and GGOH production using microscale instrumentation by LRS5 (A) and LRS6 (B). Percentage values correspond to total sugar concentration (0.2, 0.4, 2 or 4%) and values in parentheses correspond to galactose to glucose ratio. Values are mean ± standard deviation for triplicate cultivations

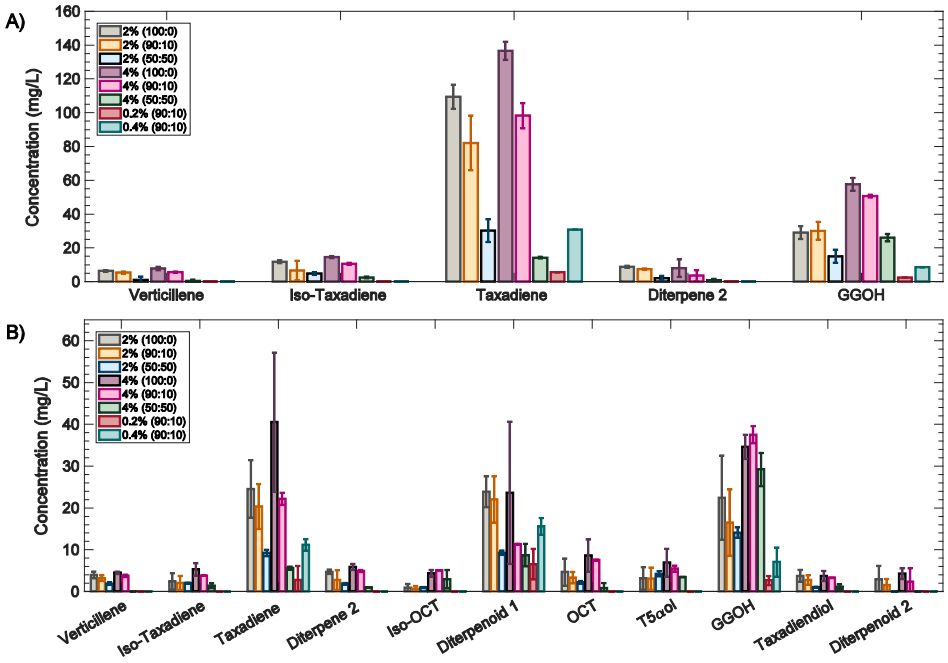

Figure 6: Initial bioreactor cultivation results. S. cerevisiae strain LRS6 was cultivated in the Applikon MiniBio 500 bioreactors in 2% (100:0) medium. A) Online process monitoring. Temperature and DO were monitored and controlled to set points of 30 °C and 30%, respectively. Medium pH was also monitored online. B) Taxane and GGOH concentration

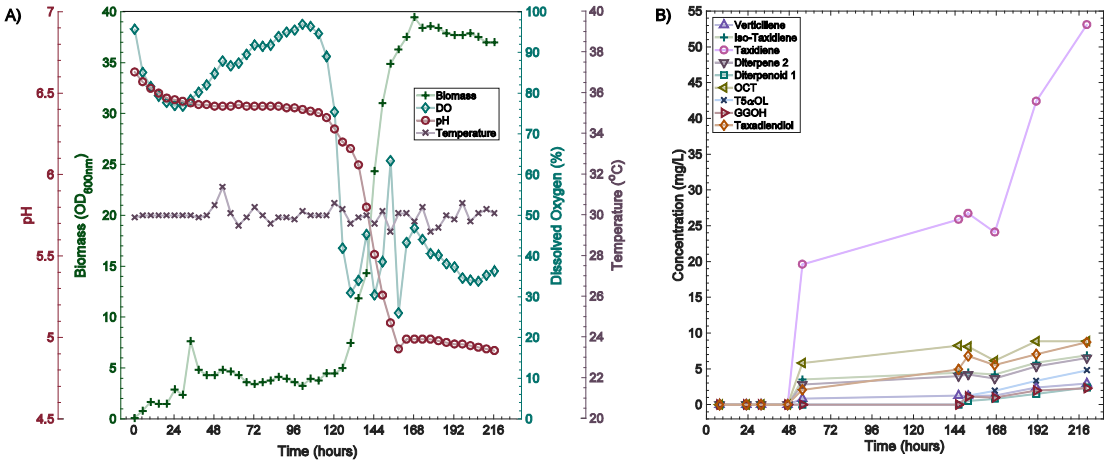

Figure 7: Effect of medium pH on LRS6 at micro and mini-bioreactor scale. A) LRS6 was cultivated in 2% (90:10) medium, both in the presence and absence of a pH 7 buffer (3 g/L potassium dihydrogen phosphate, 7 g/L disodium phosphate) in FlowerPlates at microscale. Values are mean ± standard deviation for triplicate cultivations. C) LRS6 was cultivated in the Applikon MiniBio 500 bioreactors in 2% (100:0) medium. Temperature, pH and DO were monitored online and controlled to set points of 30 °C, 6 and 30% respectively

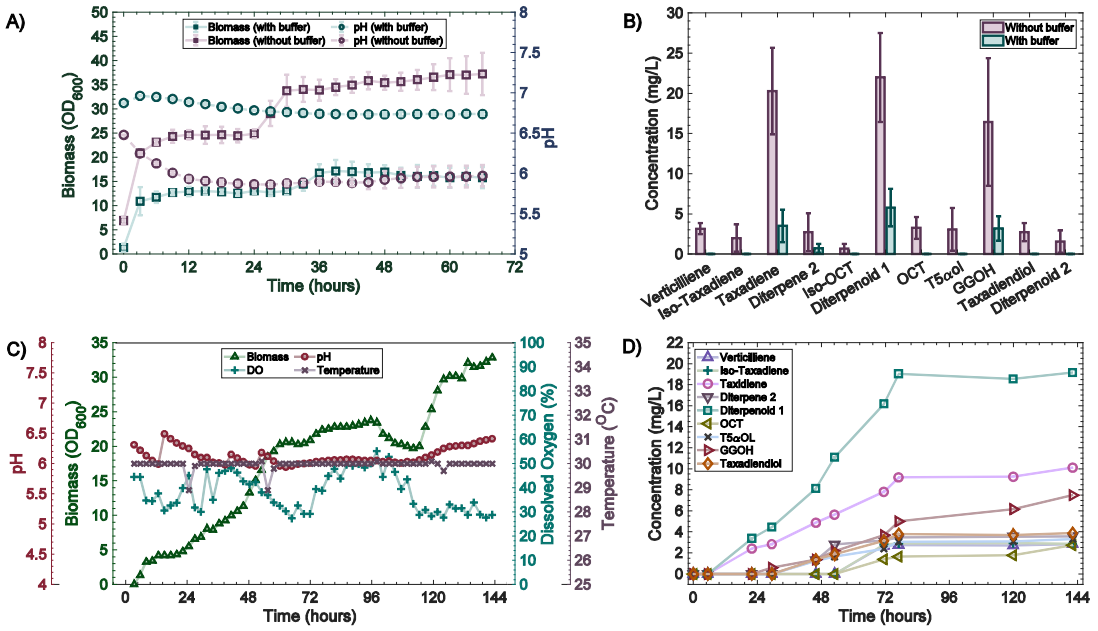

Figure 8: Characterisation in highly instrumented 1L BIOSTAT bioreactors. LRS6 was cultivated in the Applikon 1L BIOSTAT bioreactor in 2% (100:0) medium. A) Biomass, ethanol, acetate and glycerol concentration. B) Taxane accumulation kinetic summary. Non-oxygenated products included verticillene, iso-taxadiene, taxadiene, diterpene 2 and the additional unknown diterpenes. Oxygenated products included iso-OCT, diterpenoid 1, 3 and 4, OCT, T5αol and T5αAc. C) Offgas analysis summary. Oxygen uptake rate (OUR) along with ethanol and CO2 concentration was measured in the offgas online. D) Final titre of each of the taxane products

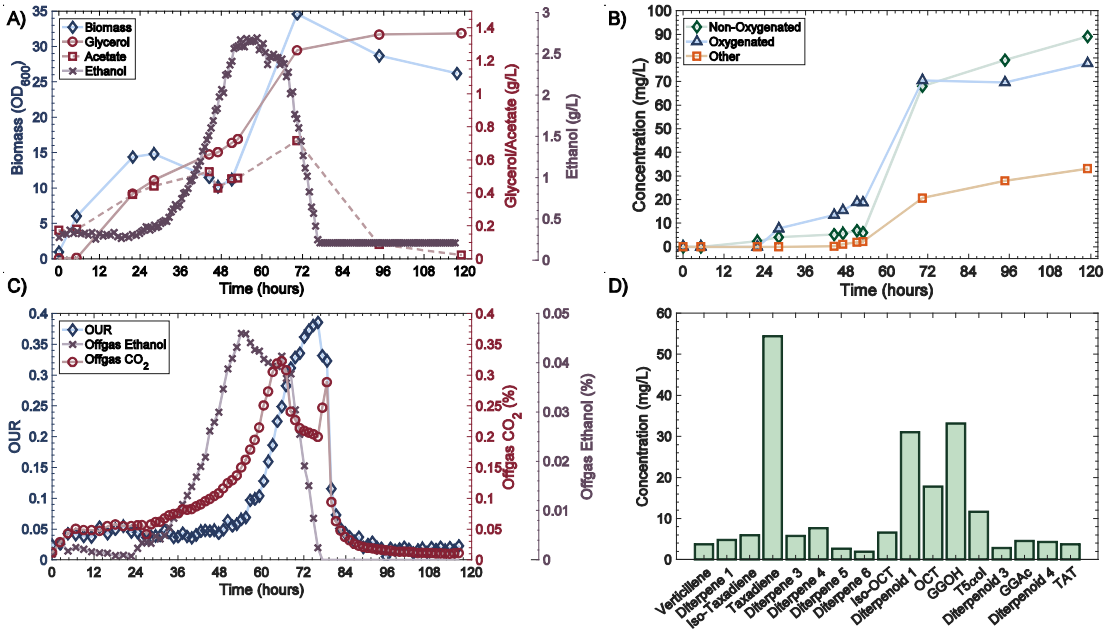

Figure 9 Selectivity of engineered taxadien-5α-ol biosynthetic pathway in S. cerevisiae across a range of scales and bioprocessing conditions. A) Yield of each product as a percentage of the total products B) Actual non-oxygenated and oxygenated taxane titres for each processing condition studied. Non-oxygenated products include verticillene, iso-taxadiene, taxadiene, diterpene 2 and the additional unknown diterpenes. Oxygenated products are iso-OCT, diterpenoid 1, 2, 3 and 4, OCT, T5αol, taxadiendiol and T5αAc. C) Actual titres of key taxol intermediates for each processing condition studied. LRS6 was cultivated at four scales, shake flask (25 mL), micro (1 mL), MiniBio 500 (250 mL) and BIOSTAT (500 mL). Bioreactor cultivations without and with pH control were performed. Yeast extract and peptone were doubled in the final pH controlled cultivation

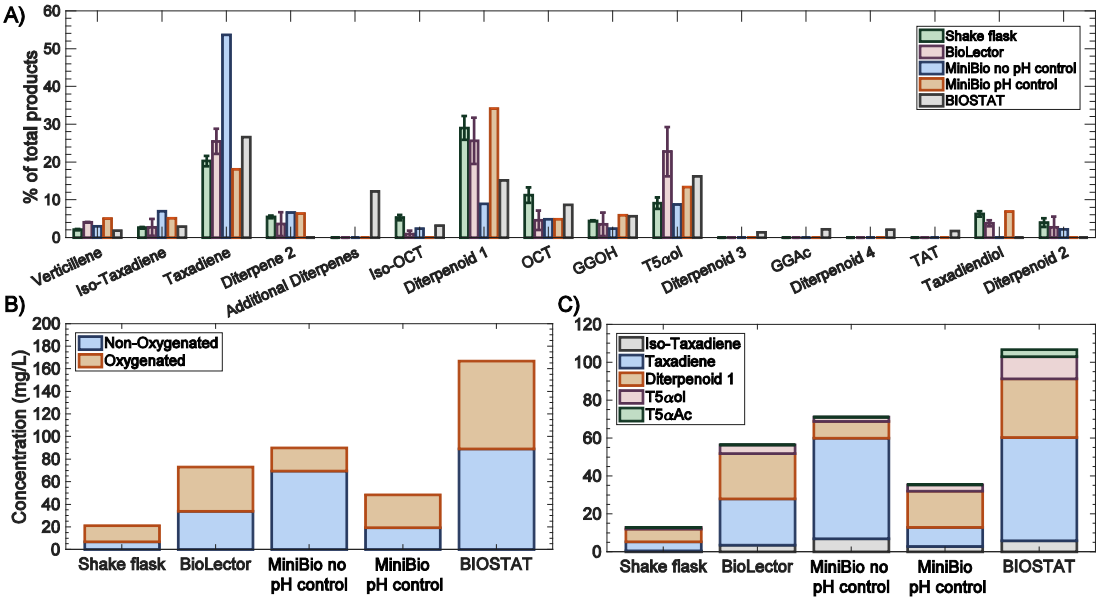

Table 1. Media compositions investigated during high- throughput screening experiments

Total sugar concentration (% *(w/v)*)	Yeast extract (g/L)	Peptone (g/L)	Ratio of glucose to galactose
2	10	20	0:100
2	10	20	10:90

2	10	20	50:50
4	10	20	0:100
4	10	20	10:90
4	10	20	50:50
0.2	10	20	10:90
0.4	10	20	10:90